Integrative and Comparative Biology Advance Access published October 29, 2016

Integrative and Comparative Biology

Integrative and Comparative Biology, pp. 1–12
doi:10.1093/icb/icw124

Society for Integrative and Comparative Biology

SYMPOSIUM

Morphological Analysis of Long Bones in Semi-aquatic Mustelids and their Terrestrial Relatives

Léo Botton-Divet,[1,†] Raphaël Cornette,* Anne-Claire Fabre,[†] Anthony Herrel,[†] and Alexandra Houssaye[†]

[†]UMR 7179, Muséum National d'Histoire Naturelle, Centre National de la Recherche Scientifique, Mécadev, 57 rue Cuvier, CP 55, Paris cedex 5 75231, France; *UMR 7205, CNRS/MNHN/UPMC/EPHE, Institut de Systématique, Évolution, Biodiversité (ISYEB), Muséum National d'Histoire Naturelle, 45 rue Buffon, Paris 75005, France

From the symposium "Functional (Secondary) Adaptation to an Aquatic Life in Vertebrates" presented at the International Congress of Vertebrate Morphology (ICVM11), June 29–July 3, 2016 at Washington, D.C.

[1]E-mail: lbottondivet@mnhn.fr

Synopsis The locomotor environment and behavior of quadrupedal mammals exert functional constraints on their limbs. Therefore long bone shapes are thought to reflect at least partially the species' locomotor ecology. Semi-aquatic species move through two media with distinct density and viscosity and their locomotor apparatus should therefore reflect a trade-off between the divergent functional constraints it faces. Adaptation to a semi-aquatic lifestyle occurred independently in otters (Lutrinae) and minks (Mustelinae). Analyzing semi-aquatic mustelids and their terrestrial relatives, we investigate long bone shape diversity, describe changes in long bone shape associated with a semi-aquatic lifestyle, and discuss the functional consequences of these shape changes. The robustness of the otter bones is highlighted and its potential ballast role discussed. Large epiphyses are observed in otters but this trend seems associated with terrestrial more than with aquatic locomotion. Thus, the most aquatic species, *Enhydra lutris*, presents narrow knee articulations compared to similar sized less aquatic species. *Enhydra lutris* presents a fore- and hind limb shape that diverge from that in other otters. Minks show bone shapes similar to each other but only *Neovison vison* tends to differ from its terrestrial relatives. The evolution of limb shape in this group is strongly correlated with size, locomotor mode, and phylogenetic history, leading to a morphological pattern where the roles of each of these factors are difficult to disentangle.

Introduction

Water and air present strong differences in density and viscosity that animals have to deal with when moving through these different media (Dejours 1987). Whereas the main external force during terrestrial locomotion is gravity, moving through water involves important drag forces while gravity is offset by buoyancy. Therefore semi-aquatic animals that move through water or on land face distinct and divergent mechanical constrains (Schmidt-Nielsen 1972; Gillis and Blob 2001). As they move extensively through both water and on land, semi-aquatic mustelids are of great interest to our understanding of the transition between land and water, though a semi-aquatic lifestyle does not necessarily mean the presence of a transitional form however (Fish 1996). The study of extant semi-aquatic mammals, in addition to providing information on the form–function relationships of these species, gives clues to understand the evolution of modern aquatic mammals with no extant semi-aquatic forms such as cetaceans and sirenians (Domning 2002; Fordyce 2002; Uhen 2007).

Here, we study the potential adaptations to a semi-aquatic environment by studying the differences in limb shape in terrestrial and more aquatic species of mustelids. In this study, we mainly focus on the long bones because they bear static as well as dynamic mechanical loads. Their shape, articulations, and the musculoskeletal system more generally determine the possible movements and the animal's performance in a given environment. Furthermore,

previous studies have shown that the evolution of limb bone shape is impacted by several entangled factors including phylogenetic heritage (Morgan 2009; Álvarez et al. 2013; Fabre et al. 2013), functional constraints (Chamay and Tschantz 1972; Bass et al. 2002; Andersson 2004; Ruff et al. 2006; Cornette et al. 2014; Rose et al. 2014; Fabre et al. 2015) as well as geometric, architectural (Gould and Lewontin 1979), and developmental constrains (Cubo 2004; Cubo et al. 2008).

We choose the Mustelidae as a model group because they display a wide ecological diversity and diverse specializations in the locomotor apparatus while including as semi-aquatic forms (Schutz and Guralnick 2007; Larivière and Jennings 2009; Fabre et al. 2015). All the extant species of the Lutrinae sub-family are semi-aquatic (Larivière and Jennings 2009) with various degrees of association to the aquatic environment. Indeed the time budget ranges from less than 20% of time spent in water for species that only hunt in water (*Lutra lutra*; Nolet and Kruuk 1989; Beja 1996) to about 100% for sea otters (*Enhydra lutris*; Larivière and Jennings 2009). Similarly, while most of the otter species hunt for elusive prey, catching them with their mouth, the sea otters (*E. lutris*) *Amblonyx* and *Aonyx* feed mainly on shellfish, urchins, or crustaceans that they catch using their paws (Bodkin 2001; Larivière 2001; Nowak 2005; Larivière and Jennings 2009).

Two semi-aquatic species are present among the Mustelinae, the sister taxon of the Lutrinae (Fig. 1); the European mink *Mustela lutreola* and the American mink *Neovison vison* are both semi-aquatic (Williams 1983a, 1983b; Youngman 1990; Lodé 1999). As they do not constitute a monophyletic group (Agnarsson et al. 2010; Sato et al. 2012; Slater et al. 2012) their semi-aquatic lifestyle is the result of independent evolutionary events. Mustelinae present, moreover, a broad range of locomotor abilities; they are able to enter the burrows of their prey but they are also skilled climbers and able swimmers (Sheffield and Thomas 1997; Larivière 1999; Veale 2013).

From a functional point of view both minks swim mainly using forelimb paddling associated with hind limb paddling at lower speed (Williams 1983a, 1983b; Lodé 1999). Otters present swimming strategies ranging from paddling with all four limbs to body and tail undulation depending on the species and swimming speed (Estes 1980; Taylor 1989; Fish 1994; Larivière 2001; Nowak 2005; Larivière and Jennings 2009). Aside from swimming, the forelimb is involved in other locomotor activities (e.g., running and climbing) as well as food seeking (digging up prey, feeling around underwater), grooming, mating, or food/item manipulation in the case of otters (Nowak 2005; Larivière and Jennings 2009; Hunter and Barrett 2011).

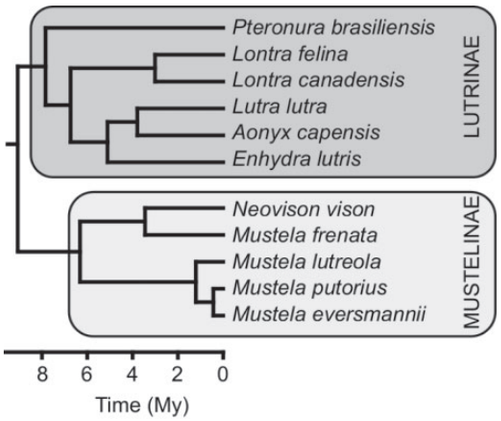

Fig. 1 Phylogeny of species used in the study based on the tree in Slater et al. (2012). Time scale in millions of years.

This study focuses on the long bones of the fore- and hind limbs in semi-aquatic mustelids and aims to: (1) describe the similarities and differences between different species of Mustelinae and Lutrinae that show different locomotor ecologies; (2) describe changes in long bone shape associated with variation in locomotor ecology; and (3) debate the functional consequences of shape changes in the light of the muscular anatomy and species ecology.

Materials and methods

Material

Eleven species of Mustelidae were selected, eight semi-aquatic and three closely related terrestrial species. We studied the humerus, ulna, radius, femur, tibia, and fibula from the left side in all specimens when available, otherwise right bones were selected and digitized bones were mirrored prior to analysis. Specimens identified as juveniles on the basis of the absence of fusion of the epiphysis, showing abnormal bone accretion or uncommon articular surface wear were excluded from the analysis. Specimens used are housed in the collections from the Muséum National d'Histoire Naturelle, Paris (MNHN); the National Museum of Natural History, Washington (NMNH); the Museum of comparative Zoology, Harvard (MCZ); the University of Alaska Museum, Fairbanks (UAM); Museum fur Naturkunde, Berlin (MFN); the Naturhistorisches Museum Basel (MHNB); and the Staatliches Museum für

Naturkunde Stuttgart (SMNS). See Supplementary Material S1 for details on specimens.

Bone digitization

Bones were digitized in three dimensions using a white light fringe Breuckmann 3D surface scanner (StereoSCAN^{3D}, 5 megapixels resolution).

Since long bones present only a few anatomical landmarks, semi-landmarks sliding on both curves and surfaces were added. This procedure detailed in Gunz et al. (2005) allows to build a spatially homologous landmarks set.

Landmarks and curves were digitized on the surfaces of the scans using the IDAV Landmark software package (Wiley et al. 2005). Curve sliding semi-landmarks were re-sampled using the algorithm detailed in Supplementary Material S2. All curves are bordered by anatomical landmarks as recommended by Gunz et al. (2005). The repeatability of anatomical landmarks was evaluated based on measurements taken five times on each of the five *Mustela frenata* specimens. These measurements were superimposed and visualized using principal component analyses (PCAs); measurement variability was smaller than inter-specimen variability. The number of each type of landmark per bone and details about anatomical landmarks and curves are given in Supplementary Material S3.

For each bone, a template was designed. A specimen was arbitrarily chosen to design the template. Surface points were manually added to this template using the IDAV Landmark software package. This template was used for the projection of surface sliding semi-landmarks onto the surface of the specimens and for the first sliding step. The process projecting surface sliding semi-landmarks form the template onto specimen surface is detailed in the documentation of the "placePatch" function of the Morpho package (Schlager 2013).

Curve and surface sliding semi-landmarks were slid minimizing bending energy of a Thin Plate Spline (TPS) between the specimen and the template as a first step and then three times between the result of the previous step and the Procrustes consensus of the dataset, according to the procedure given in Gunz et al. (2005) using the package Morpho (Schlager 2013) in the R environment (R Core Team 2014) as detailed in Botton-Divet et al. (2015).

Morphometrics

Specimens were superimposed using a Generalized Procrustes Analysis (GPA) (Gower 1975; Rohlf and Slice 1990) to isolate size from shape and remove the effect of relative position of specimens in the coordinate system while comparing them. The GPA was performed using the Rmorph package (Baylac 2013) in R (R Core Team 2014). Following GPA, distributions of superimposed datasets were visualized by performing PCA on superimposed coordinates projected onto tangent space as provided by the "gpa" function of the Rmorph package (Baylac 2013). Shapes associated with both sides of the PCA axes were computed and used as fixed points to compute a TPS deformation of the template mesh using the "Morpho" (Schlager 2013) package for visualization purpose.

Results

Humerus

The first two axes of the PCA performed on the shape data of the humerus (Fig. 2A) represent 71.6% of the total variance. The first axis describes the differences between Mustelinae (negative side) and Lutrinae (positive side). The three closely related *Mustela* species, *M. lutreola*, *M. putorius*, and *M. eversmannii*, are spread along the second axis. *Mustela eversmannii* has the highest scores. The two minks, *M. lutreola* and *N. vison*, are positioned close to one another. Specimens with positive scores on the first axis show more robust bones with expanded epiphyses; a more curved diaphysis at the middle with an expansion of the cranial side between the greater trochanteric crest and the deltoid crest; an expanded greater and lesser trochanter; a wider lateral epicondylar crest that is more expanded laterally and starts more proximally; a capitulum that is larger and a medial epicondyle that is expanded toward the caudo-medial direction and proximally in comparison to species in the negative side of the first axis that display the opposite shape. Specimens on the negative side of the second axis (Fig. 3A) present a more proximally curved humerus; a humeral head that is more elongated antero-posteriorly leading to a less rounded shape in contrast to species that are on the negative part that show a lesser trochanter expended on its distal point, a lateral epicondylar crest projected more anteriorly, a medial epicondyle expanded medially, and the capitulum going more distally.

Ulna

The first two axes of the PCA performed on the ulna shape data (Fig. 2B) represent 74.2% of the total variance. The first axis describes the differences between *E. lutris* (negative side) and all other species (positive side). The second axis separates the

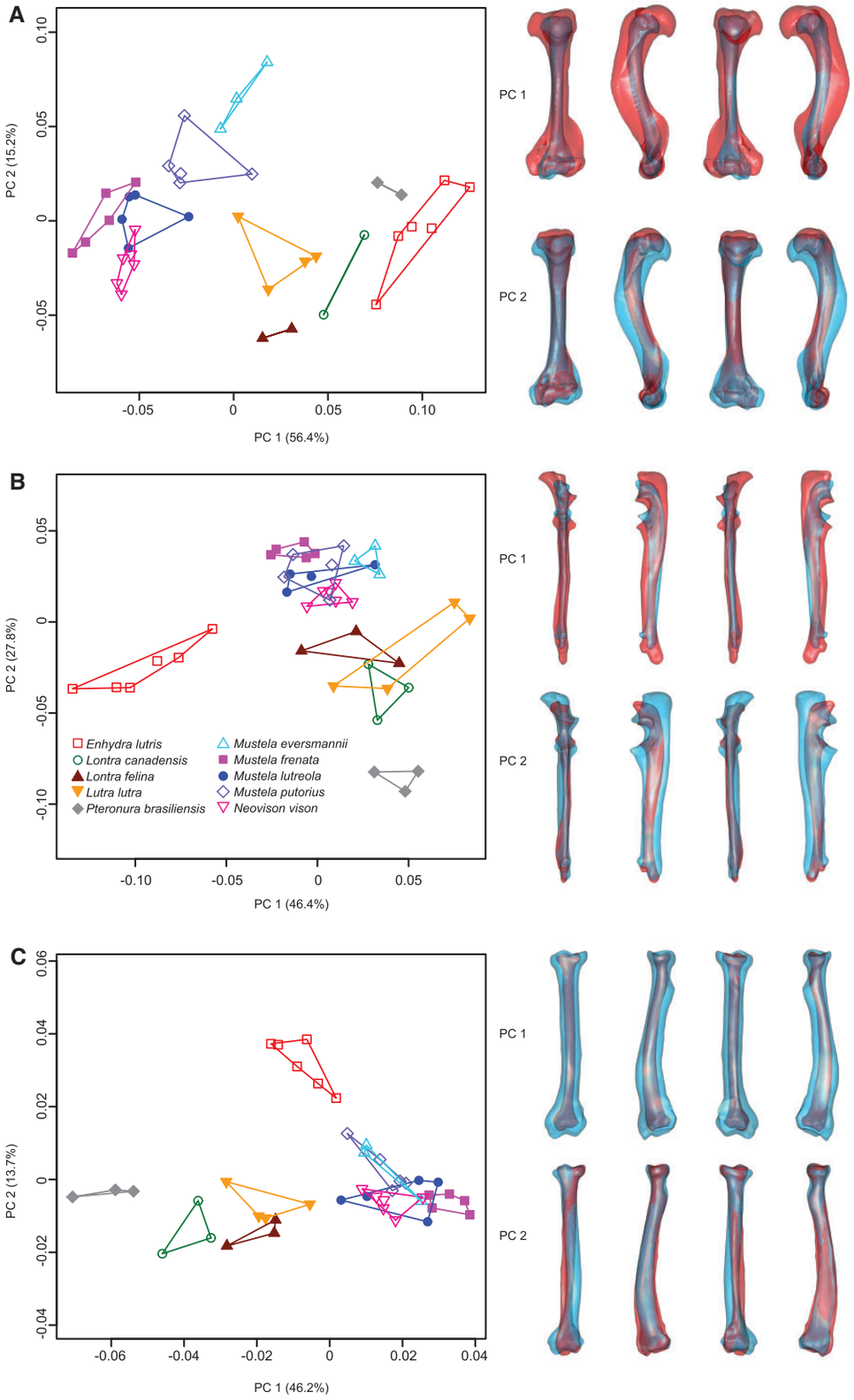

Fig. 2 Results of the PCAs performed on the morphometric data of the (**A**) humerus; (**B**) ulna; (**C**) radius. Shape changes associated with each extreme of the first two principal components are represented: blue, negative extreme of the axis; red, positive extreme of the axis. Bones are represented form left to right in cranial, lateral, caudal, and medial views.

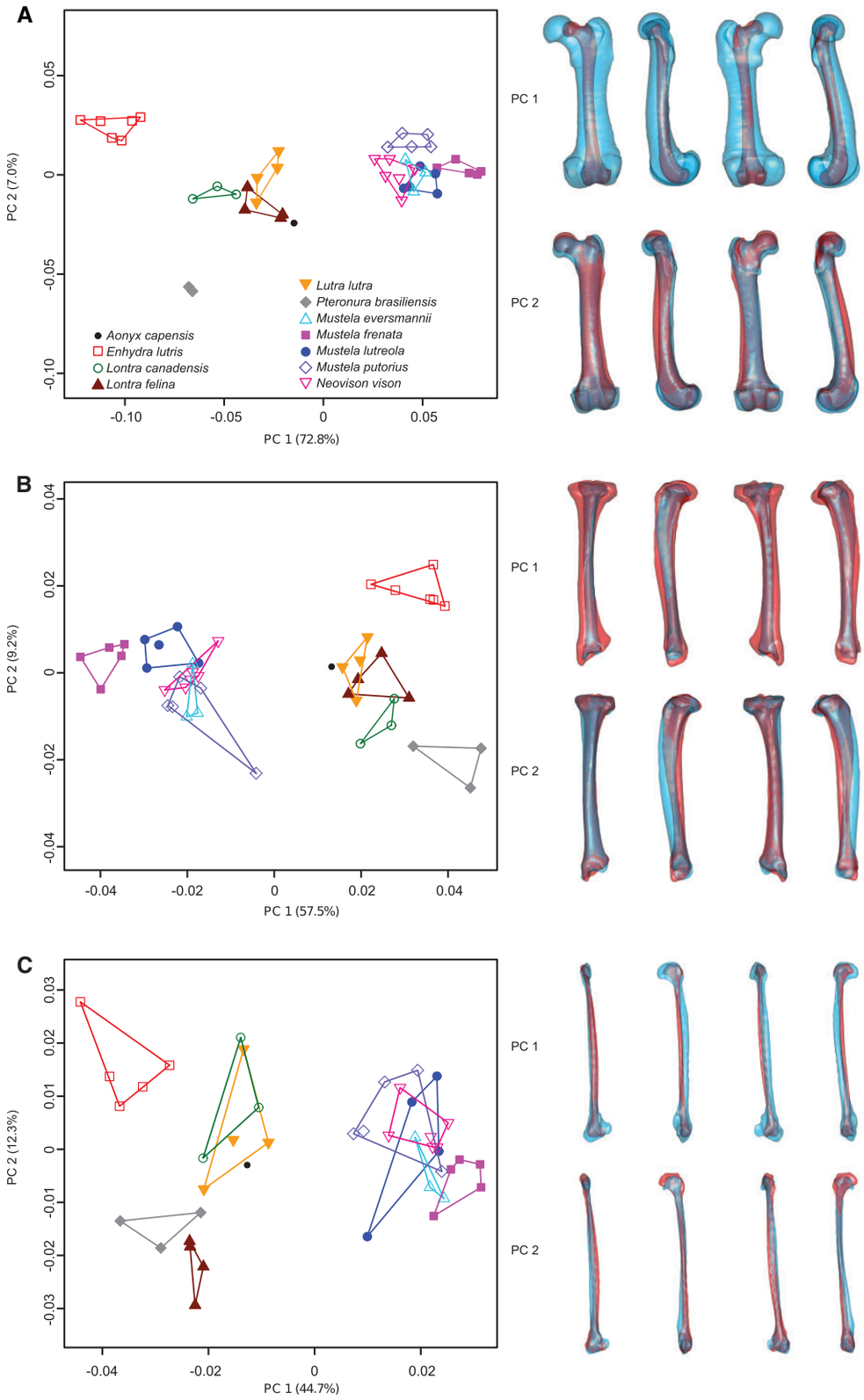

Fig. 3 Results of the PCAs performed on the morphometric data of the: (**A**) femur; (**B**) tibia; and (**C**) fibula; shape changes associated with each extreme of the first two principal components are represented: blue, negative extreme of the axis; red: positive extreme of the axis. Bones are represented form left to right in cranial, lateral, caudal, and medial views.

Lutrinae on the negative side from the Mustelinae on the positive side. In each of these sub-families there is a spread of the species along the second axis. When compared with specimens on the negative side of the first axis, specimens on the positive side tend to present a more robust ulna with a more curved diaphysis and a styloid process that is oriented toward the palmar side; an olecranon process that is curved toward the latero-medial direction; a *m. pronator quadratus* insertion ridge that runs until the middle of the diaphysis; a medial coronoid process that is oriented distally providing a wider opening of the trochlear notch; a laterally expanded proximo-lateral lip of the trochlear notch and the lateral coronoid process. The second axis of the PCA on the ulna separates species with a robust ulna (negative side of the axis) from species with a slender ulna (positive side of the axis). This robustness is especially developed in the antero-posterior direction, forming a laterally flattened ulna. Species with the lowest scores tend to have a large olecranon process with an expansion of the proximo-palmar extremity toward the medio-palmar direction; a medial coronoid process that is more expanded; an anconeus process that is more expanded toward the cranial direction; and the proximal lips of the trochlear notch are more expanded medially and laterally. In contrast, species with the highest scores on the second axis present a sharper *m. pronator quadratus* insertion ridge.

Radius

The first two axes of the PCA performed on morphometric data of the radius (Fig. 2C) account for 59.9% of the total variance. The first axis of the PCA on the radius separates the Lutrinae on the negative side of the axis from the Mustelinae on the positive side of the axis. The second axis separates *E. lutris* from other species. Additionally *M. eversmannii* and *M. putorius* tend to be separated from *N. vison* and *M. lutreola* and show slightly higher scores on the second axis. Species with low scores on the first axis have a more robust radius with a diaphysis that is expanded at its distal part; at the latero-cranial side and the epiphyses are larger; surfaces that articulate with both humerus and the ulna are larger; the radial tuberosity is located more distally and the styloid process expands more distally. In contrast, specimens with low scores on the first axis display the opposite shape with the ulno-radial distal articular surface larger and oriented more toward the palmar direction. Specimens with high scores on the second axis present a torsion of the diaphysis producing a change in the alignment of the two epiphyses and a smaller proximal contact area with the capitulum than specimens with low scores that display the opposite morphology.

Femur

The first two axes of the PCA performed on the femur shape (Fig. 3A) represent 79.8% of the total variance. The first axis separates Mustelinae on the positive side from Lutrinae on the negative side. Among Lutrinae, *E. lutris* and *Pteronura brasiliensis* have the highest scores, followed by *Lontra canadensis*. The three other species present similar scores. The first axis tends to separate *N. vison* from *M. frenata* that has the lowest scores of all species. The second axis separates *E. lutris* on the positive side of the axis from *P. brasiliensis* on the negative side. Additionally, *Mustela putorius* presents higher values on the second axis than the other Mustelinae. Specimens on the negative side of the first axis present more robust bones with proportionally larger epiphyses with a distal epiphysis winding more on its caudal part and a diaphysis that is slightly more curved toward the cranial side, whereas specimens on the positive side of the first axis display the opposite morphology. Specimens on the negative side of the second axis show a femoral head that is oriented more cranio-medially, a greater trochanter that is expanded more dorso-medially, wider distal articular condyles along the mediolateral axis, and lips of the trochlea that are more prominent in addition to having wider epicondyles. Furthermore, the greater trochanter of these specimens is more expanded laterally in its most proximal part, whereas it is more expanded in its distal part in specimens with high scores. The latter also present a diaphysis that is more curved toward the cranial direction in the middle of the diaphysis and a cranial greater trochanter crest that is expanded more distally.

Tibia

The first two axes of the PCA performed on the tibia data (Fig. 3B) represent 66.7% of overall variance. The first axis separates Mustelinae on the negative side of the axis from the Lutrinae. Low scores on this axis separate *M. frenata* from *N. vison*. The Lutrinae are spread along the second axis, *E. lutris* presents the highest value while *P. brasiliensis* shows the lowest one, followed by *L. canadensis*. The second axis also tends to separate *M. lutreola* from *M. putorius* and *M. eversmannii* that have lower scores. Specimens on the positive side of the first axis have more robust tibia with relatively larger

Table 1 Pearson's product moment correlation tests between centroid size (Log10) and the two first principal components of each bone. Significant results are in bold.

		r	*t*	df	*P*
Humerus	**PC1**	**0.90**	**12.88**	**38**	**<0.01**
	PC2	−0.29	−1.86	38	0.07
Ulna	PC1	−0.24	−1.58	40	0.12
	PC2	**−0.84**	**−9.65**	**40**	**<0.01**
Radius	**PC1**	**−0.78**	**−7.86**	**41**	**<0.01**
	PC2	**0.47**	**3.37**	**41**	**<0.01**
Femur	**PC1**	**−0.92**	**−15.25**	**42**	**<0.01**
	PC2	−0.08	−0.52	42	0.60
Tibia	**PC1**	**0.92**	**15.41**	**43**	**<0.01**
	PC2	0.13	0.84	43	0.40
Fibula	**PC1**	**−0.91**	**−13.91**	**41**	**<0.01**
	PC2	0.18	1.21	41	0.23

epiphyses. The diaphysis is more curved particularly on the lateral and cranial sides. While the cranial maximum of curvature of the specimens with low scores occurs around the proximal first quarter of the bone, it is located in the middle of the diaphysis in specimens with high scores. The second axis separates specimens with single antero-posterior curvature and a ''bow like'' tibia on the negative side from specimens with a double ''S''-like curvature with a diaphysis that is also curved toward the medial side in its middle. Additionally, specimens on the negative side tend to have a longer cranio-medial tip of the distal articular facet and a more squared medial malleolus with the cranial tip slightly shifted caudally as compared to specimens on the positive side.

Fibula

The first two axes of the PCA on the fibula (Fig. 3C) account for 67.7% of the overall variance. The first axis separates Mustelinae from Lutrinae. Lutrinae are spread along the second axis, with *E. lutris* presenting the highest scores, followed by *L. canadensis*, *Lontra felina*, and *Aonyx capensis*. On the negative side of the axis *L. felina* presents the lowest values followed by *P. brasiliensis*. Specimens on the negative side of the first axis tend to display a larger epiphysis and a diaphysis that is more curved toward the caudal direction in its middle. In contrast, specimens with high scores show a distal tip of the fibula that is less expanded distally leading to an epiphysis with a distal margin that is perpendicular to the main axis of the bone. On the second axis, specimens with positive scores present a large proximal epiphysis rotated toward the caudal direction, a round lateral malleolus, a short distal facet that articulates with the tibia, and a proximal facet articulating with the tibia small and oriented toward the proximal direction. On the negative side specimens have a squared lateral malleolus and a distal facet that articulates with the tibia expending toward the proximal direction.

For all bones but the ulna the first PC is significantly correlated with the logarithm of the centroid size (Table 1). For the ulna, centroid size is only significantly correlated with the second PC. Additionally, the second axis of the PCA is also significantly correlated with the centroid size for the radius.

Discussion

The pattern displayed by all the PCAs is rather similar. The difference between Mustelinae and Lutrinae is the main driver of the pattern as it appears on the first PC for all bones except the ulna where this separation appears on the second axis. The humerus presents the most particular pattern with Lutrinae and Mustelinae occupying a similar sized area of the morphospace. For all the other bones, Lutrinae occupy a larger area of the morphospace. This higher shape diversity among Lutrinae may be related to the large evolutionary and ecological diversity of this group. Even if all species are semi-aquatic the amount of time they spend in water differs as does the way they swim, their food, and the environment they face depending on the species. Mustelinae included in our dataset all live in temperate areas with differences in cold exposure and water availability. Among otters some species catch elusive prey (fish) whereas others harvest crustaceans. All Mustelinae hunting for elusive prey at some time enter burrows. Therefore there is a difference in the diversity of environment and constraints faced by Lutrinae compared with Mustelinae that could be at the origin of the difference in the area of the morphospace occupied by the two groups.

The morphospace for the Lutrinae is different between the lower arm of the forelimb and the hind limb. In the lower arm, only *E. lutris* separates from its relatives with all other species spread along a single axis correlated to size. As *E. lutris* displays very unique manipulative skills and rarely walks on land compared with the other Lutrinae, its divergence was expected. The other Lutrinae do not seem to display a specialization of the lower arm different from that caused by allometry. Hind limb bones present a quite similar pattern for all bones. Whereas the forelimb is used for locomotion but also

food/item manipulation, grooming, or mating, the hind limb is mainly used for locomotion. The first axis of the PCA on hind limb bones is correlated with size, the second axis, however, presents diversity among Lutrinae not linked to size. *Enhydra lutris* appears on one side of the axis diverging from the other otters and Mustelinae as it was observed by Mori et al. (2015) for hind limb muscles and linear measurements of bones. The other side of this axis is occupied by *P. brasiliensis*, plus *L. felina* in the case of the fibula. Aside from the size difference, a functional or ecological interpretation of the difference in hind limb bone shape between *Pteronura* and the other four limb swimming otters requires further investigations.

Lutrinae differ from their sister taxa Mustelinae in the robustness of their bones and their relatively larger epiphysis as noticed in previous studies (Fabre et al. 2013, 2015; Samuels et al. 2013). This tendency is observed in all bones and is visible on the first axis of the PCA on all bones except the ulna where it appears on the second axis. The axes separating Lutrinae from Mustelinae are correlated with the centroid size of the bones. Therefore it appears that size-related shape changes are one of the factors shaping the divergence between the two sub-families. As body mass increases, mechanical loads on the limb bones increase (Garcia and Dasilva 2006) leading to allometric changes. Joint stability is achieved through an augmentation of the load transfer surface (articular surfaces) as well as postural changes (Biewener 1983; Doube et al. 2009).

Size may be differently constrained in Mustelinae and Lutrinae. Water imposes constraints on the maintenance of body temperature since heat loss is higher in water than in air (Downhower and Blumer 1988; Innes and Lavigne 1989) and may thus constrain an animal's size (Downhower and Blumer 1988; Clauset 2013). Indeed, the surface over volume ratio decreases when size increases and consequently the cost of maintaining body temperature decreases when animal gets larger (Schmidt-Nielsen 1984). This effect is particularly strong in animals such as mustelids that have long and thin bodies with a high surface to volume ratio (Brown and Lasiewski 1972; King 1989). However, most Mustelinae are said to be adapted to enter burrows in search of prey or shelter. Therefore the diameter of the prey burrow is said to be a constraint acting on the size of the Mustelinae and could be a reason of their long and thin body shape (Brown and Lasiewski 1972; Moritz et al. 2007; Horner and Biknevicius 2010).

Furthermore, an increase in bone robustness could be linked with a ballast role if associated with an increased inner bone compactness. Fish and Stein (1991) highlighted the link between limb bone density and the time spent in water as well as time spent diving in mustelids. Additionally, Nakajima and Endo (2013) showed that the medullar cavity at the center of ossification is smaller in *L. lutra* and *E. lutris* (and thus the compact cortex proportionally thicker) than in terrestrial relatives of similar size (*Gulo gulo* and *Meles meles*). This suggests that the increased robustness of the appendicular skeleton in Lutrinae may be a way to reduce positive buoyancy and therefore to limit energy consumption while diving (Taylor 1994). Additionally, the fact that this bone density increase is located in the appendicular skeleton could play a role in underwater stability as suggested by Fish and Stein (1991) by inducing a shift of the center of mass ventrally.

In our dataset bone curvature seems to increase with animal size for the humerus, femur, tibia, and fibula. Higher curvature implies higher bending moment on the bone. Therefore the global trend among quadrupedal mammals is to show straighter bones in larger animals (Biewener 1983). Nevertheless, using a larger sample of mammals (Bertram and Biewener 1992) showed that the variability of curvature at a given body mass was large in humerus and femur, and that the curvature of these bones is not *per se* correlated to body mass. Three hypotheses were suggested to explain bone curvature: (1) the accommodational hypothesis stating that bone is modeled by the pressure of surrounding tissues such as muscle bellies on the periosteum; (2) the bone strain hypothesis stating that the surrounding musculature compensates for the bending moment leading to a system equivalent to an axially loaded bone (Lanyon 1980); and (3) Bertram and Biewener (1988) suggested that bone curvature permits a certain predictability of the mechanical stresses orientation.

The expanded cranial part of the humerus diaphysis associated with a more distal convergence of the greater trochanter and deltoid crests means more distal and cranial insertions of the shoulder abductors such as the *m. deltoideus* and flexors such as the *m. pectoralis major* and the *m. pectoralis minor* (Fisher 1942; Howard 1973; Ercoli et al. 2014). This antero-distal displacement of the shoulder retractors implies an extended in-lever and therefore a slower but more powerful retraction of the shoulder. This is in accordance with an adaptation to a denser medium such as water. Nevertheless this pattern is observed in *E. lutris* that does not use its forelimb for

swimming, suggesting the functional roles underlying the development of this feature may be more complex. On the caudal side of the bone the curvature leaves a large space for the belly of muscles such as the *m. triceps brachii*. The lesser trochanter of the humerus which is expanded medially in Lutrinae, is the area of insertion of *m. subscapularis* insertion, a rotator of the humerus. The distal epiphysis is particularly expanded in Lutrinae as noted by Schutz and Guralnick (2007) and Fabre et al. (2015) providing a stable insertion for the forearm. The lateral epicondylar crest is wide and originates more proximally than in Mustelinae. This crest provides the origin for the *m. anconeus*, which is an elbow extensor on the caudal side, and provides the origin for several digital and carpal extensors on its latero-cranial side. These muscles are involved in elbow extension and wrist movements and may therefore play a role during swimming as suggested by Ercoli et al. (2012). The elongated olecranon process of the ulna in Lutrinae produces a longer in-lever for the elbow extensors (*m. triceps brachii*, *m. anconeus*). Additionally the expansion of the olecranon toward the medial and caudal sides produces an insertion point for the *m. triceps brachii caput longus* farther from the rotation point, thus providing a greater in-lever even when the elbow is extended (Van Valkenburgh 1987). As *E. lutris* does not use its forelimb for propulsion it seems difficult to determine if the expansion of the lateral epicondylar crest results from an adaptation to aquatic locomotion or to the increased mechanical load while walking on land.

The small *m. pronator quadratus* insertion ridge observed in *E. lutris* as compared to other Lutrinae, as well as the small olecranon process may be related to the fact that this species does not use the forepaw for swimming. As a consequence the requirement for strong pronator and elbow extensor may be reduced in this species.

The expanded latero-cranial part of the diaphysis in Lutrinae radius may correspond to an enlarged insertion of the *m. supinator*. Additionally the more curved shape of the radius leads to an insertion area for the *m. supinator* farther from the rotation axis of the radius on the ulna and therefore to a better in-lever for this muscle to supinate the forearm. This could be related to the manipulative behavior of Lutrinae (Hall and Schaller 1964; Iwaniuk et al. 2000).

The femur of Lutrinae is slightly more curved, moving cranially the insertion of the *m. vastus medialis* and *m. vastus lateralis*. These muscles are knee extensors that could be related to thrust production. The wide distal epicondyles in the femur of *P. brasiliensis* provide a stable knee articulation while *E. lutris* has narrower and rounder epicondyles. As *P. brasiliensis* has a more terrestrial lifestyle than *E. lutris* the constraint of stability of the knee joint may indeed be higher in *Pteronura*. The narrow and round distal epicondyles in *Enhydra* associated with the absence of a *fovea capitis* on the femoral head suggest greater degrees of freedom in the femur articulation. Additionally, *E. lutris* displays a femoral neck forming a more obtuse angle with the main axis of the diaphysis than in *Pteronura*. This feature could be related to a reduction in bending moment while the bone is axially loaded or to a larger in-lever for hip muscles. This latter hypothesis is supported by the presence of a greater trochanter expanding more distally and the extensive use of the hind limbs for swimming.

The expanded contact surfaces between fibula and tibia observed in *L. felina* and *P. brasiliensis* suggest a reduction of mobility of these articulations and therefore the ankle.

The two minks occur in the same area of the morphospace for all bones except the humerus. Nevertheless Mustelinae species overlap rather strongly in the morphospace suggesting that their relative proximity should be interpreted with some caution. Only *N. vison* separates visibly from *M. frenata* but this difference matches the size difference between the species and therefore allometry and function cannot be separated. The shape of the humerus tends to separate the minks from their terrestrial relatives and to pool them. This could be a convergence of the two minks in humeral shape associated with their semi-aquatic lifestyle. Indeed, the forelimb is preferentially used for swimming in minks (Larivière 1999; Lodé 1999) suggesting a stronger functional pressure linked to an aquatic locomotion for the forelimb.

Conclusion

Divergence between Mustelinae and Lutrinae is marked in all long bones. This divergence matches the difference in body size between the two groups. While most species seem to follow a similar allometric pattern for shape of the lower arm long bones of the forelimb, *E. lutris* displays a distinct ulnar and radial shape with a slender and curved ulna and a bending of the radius toward medial direction. When considering the hind-limb, *E. lutris* presents long bones that differ from all other Lutrinae species, including *P. brasiliensis* that is of similar size. The forelimb lower arm and hind limb present unique characteristics that we suggest to be linked to the manipulative behavior; the exclusive use of the

hind limb for aquatic locomotion and the rarity of terrestrial locomotion in *E. lutris*. *Pteronura brasiliensis* displays hind limb bone shapes that are divergent from those in the other otter species in this dataset with a specific femur and tibia curvature, a femoral head that is perpendicular to the main bone, with a wide knee articulation. We hypothesize that the large size of this species leads to its separation from the other four-limb swimming otters.

Semi-aquatic Mustelinae present long bone shapes that are more similar to the terrestrial species of the sub-family. *Neovison vison* tends to separate from its closest terrestrial relative *M. frenata*, but the direction of this difference does not differ from the expected allometry when considering the size difference between the two species. Even if the two minks occur in the same area of the morphospace for all bones, they do not separate distinctly from their relatives. Assessment of potential convergence between these species and with the Lutrinae as a whole requires further investigations.

Future investigations should study the potential changes in limb segment proportions and patterns of covariation between the different locomotor groups among mustelids to determine if changes in ecology lead to differential specialization of each limb or limb segments. Moreover, a larger number of species should allow to produce a robust phylogenetic framework for these analyses.

Acknowledgments

The authors want to thank all the collection curators for the loan of the specimens. S. Peurach of the NMNH; J.M. Chupasko of the MCZ, Harvard; L. Costeur of the MHNB, Basel; C. Funk and F. Mayer of the MFN, Berlin; L.E. Olson and A. Gunderson of the UAM, Fairbanks; G. Véron, J. Cuisin, J. Villemain, and C. Bens of the MNHN, Paris; S. Merker of the SMNS, Stuttgart. The authors would like to thank D. Polly of the Indiana University, Bloomington, and an anonymous reviewer who provided valuable and constructive comments that improved the original manuscript and provided interesting suggestions for future analyses. The authors thank the platform for morphometrics of the UMS 2700 (CNRS, MNHN) for access to the surface scanner.

Funding

This work was supported by the doctoral school "Frontières du vivant" and the Bettencourt Schueller foundation [to L.B.-D.]; The Agence Nationale de la Recherche [ANR-13-PDOC-0011 to L.B.-D., Al.H., and An.H.] [to L.B.-D., Al.H., and An.H.]; and the Marie-Skłodowska Curie fellowship [EU project 655694—GETAGRIP to A.-C.F.].

Supplementary material

Supplementary data available at *ICB* online.

References

Agnarsson I, Kuntner M, May-Collado LJ. 2010. Dogs, cats, and kin: a molecular species-level phylogeny of Carnivora. Mol Phylogenet Evol 54:726–45.

Álvarez A, Ercoli MD, Prevosti FJ. 2013. Locomotion in some small to medium-sized mammals: a geometric morphometric analysis of the penultimate lumbar vertebra, pelvis and hindlimbs. Zoology 116:356–71.

Andersson KI. 2004. Elbow-joint morphology as a guide to forearm function and foraging behaviour in mammalian carnivores. Zool J Linn Soc 142:91–104.

Bass SL, Saxon L, Daly RM, Turner CH, Robling AG, Seeman E, Stuckey S. 2002. The effect of mechanical loading on the size and shape of bone in pre-, peri-, and postpubertal girls: a study in tennis players. J Bone Miner Res 17:2274–80.

Baylac M. 2013. Rmorph, a morphometrics library for R. Available from the author.

Beja PR. 1996. Temporal and spatial patterns of rest-site use by four female otters *Lutra lutra* along the south-west coast of Portugal. J Zool 239:741–53.

Bertram JE, Biewener AA. 1988. Bone curvature: sacrificing strength for load predictability? J Theor Biol 131:75–92.

Bertram JE, Biewener AA. 1992. Allometry and curvature in the long bones of quadrupedal mammals. J Zool 226:455–67.

Biewener AA. 1983. Allometry of quadrupedal locomotion: the scaling of duty factor, bone curvature and limb orientation to body size. J Exp Biol 105:147–71.

Bodkin JL. 2001. Sea otters. In: Steele, J., editor. Encyclopedia of ocean sciences. Academic Press London. p. 2614–21.

Botton-Divet L, Houssaye A, Herrel A, Fabre A-C, Cornette R. 2015. Tools for quantitative form description: an evaluation of different software packages for semi-landmark analysis. PeerJ 3:e1417.

Brown JH, Lasiewski R. 1972. Metabolism of weasels: the cost of being long and thin. Ecology 53:939.

Chamay A, Tschantz P. 1972. Mechanical influences in bone remodeling. Experimental research on Wolff's law. J Biomech 5:173–80.

Clauset A. 2013. How large should whales be? PLoS One 8:e53967.

Cornette R, Tresset A, Herrel A. 2014. The shrew tamed by Wolff's law: do functional constraints shape the skull through muscle and bone covariation? J Morphol 276:301–9.

Cubo J. 2004. Pattern and process in constructional morphology. Evol Dev 6:131–3.

Cubo J, Legendre P, De Ricqlès A, Montes L, De Margerie E, Castanet J, Desdevises Y. 2008. Phylogenetic, functional, and structural components of variation in bone growth rate of amniotes. Evol Dev 10:217–27.

Dejours P. 1987. Comparative physiology: life in water and on land. Springer Science & Business Media. Berlin.
Domning D. 2002. Sirenian evolution. In: Perrin, W, Würsig B and Thewissen J, editors. Encyclopedia of marine mammals. London: Academic Press. p. 1083–86.
Doube M, Conroy AW, Christiansen P, Hutchinson JR, Shefelbine S. 2009. Three-dimensional geometric analysis of felid limb bone allometry. PLoS One 4:e4742.
Downhower JF, Blumer LS. 1988. Calculating just how small a whale can be. Nature 335:675.
Ercoli MD, Álvarez A, Stefanini MI, Busker F, Morales MM. 2014. Muscular anatomy of the forelimbs of the lesser grison (*Galictis cuja*), and a functional and phylogenetic overview of Mustelidae and other Caniformia. J Mamm Evol 22:57–91.
Ercoli MD, Prevosti FJ, Álvarez A. 2012. Form and function within a phylogenetic framework: locomotory habits of extant predators and some Miocene Sparassodonta (Metatheria). Zool J Linn Soc 165:224–51.
Estes JA. 1980. *Enhydra lutris*. Mamm Species 133:1–8.
Fabre A-C, Cornette R, Goswami A, Peigné S. 2015. Do constraints associated with the locomotor habitat drive the evolution of forelimb shape? A case study in musteloid carnivorans. J Anat 226:596–610.
Fabre A-C, Cornette R, Peigné S, Goswami A. 2013. Influence of body mass on the shape of forelimb in musteloid carnivorans. Biol J Linn Soc 110:91–103.
Fish FE. 1994. Association of propulsive swimming mode with behavior in river otters (*Lutra canadensis*). J Mamm 75:989.
Fish FE. 1996. Transitions from drag-based to lift-based propulsion in mammalian swimming. Am Zool 36:628–41.
Fish FE, Stein B. 1991. Functional correlates of differences in bone density among terrestrial and aquatic genera in the family Mustelidae (Mammalia). Zoomorphology 110: 339–45.
Fisher EM. 1942. The osteology and myology of the California river otter. Stanford University Press: Stanford.
Fordyce R. 2002. Cetacean evolution. In: Perrin, W, Würsig B and Thewissen J, editors. Encyclopedia of marine mammals. London: Academic Press. p. 214–20.
Garcia G, Dasilva J. 2006. Interspecific allometry of bone dimensions: a review of the theoretical models. Phys Life Rev 3:188–209.
Gillis GB, Blob RW. 2001. How muscles accommodate movement in different physical environments: aquatic vs. terrestrial locomotion in vertebrates. Comp Biochem Physiol A Mol Integr Physiol 131:61–75.
Gould SJ, Lewontin RC. 1979. The spandrels of San Marco and the Panglossian paradigm: a critique of the adaptationist programme. Proc R Soc Lond B Biol Sci 205:581–98.
Gower JC. 1975. Generalized procrustes analysis. Psychometrika 40:33–51.
Gunz P, Mitteroecker P, Bookstein FL. 2005. Semilandmarks in three dimensions. In: Denis S, editor. Modern morphometrics in physical anthropology. New York: Springer. p. 73–98.
Hall KRL, Schaller GB. 1964. Tool-using behavior of the California sea otter. J Mamm 45:287–98.
Horner AM, Biknevicius AR. 2010. A comparison of epigean and subterranean locomotion in the domestic ferret (*Mustela putorius furo*: Mustelidae: Carnivora). Zoology 113:189–97.
Howard LD. 1973. Muscular anatomy of the forelimb of the sea otter (*Enhydra lutris*). Proc Calif Acad Sci 39: 411–500.
Hunter L, Barrett P. 2011. Carnivores of the world. Princeton: Princeton University Press.
Innes S, Lavigne D. 1989. Size of aquatic endotherms. Nature 341:192.
Iwaniuk AN, Pellis SM, Whishaw IQ. 2000. The relative importance of body size, phylogeny, locomotion, and diet in the evolution of forelimb dexterity in fissiped carnivores (Carnivora). Can J Zool 78:1110–25.
King CM. 1989. The advantages and disadvantages of small size to weasels, *Mustela* species. In: Gittleman JL, editor. Carnivore behavior, ecology, and evolution. New York: Springer. p. 302–34.
Lanyon LE. 1980. The influence of function on the development of bone curvature. An experimental study on the rat tibia. J Zool 192:457–66.
Larivière S. 1999. *Mustela vison*. Mamm Species 608:1–9.
Larivière S. 2001. *Aonyx capensis*. Mamm Species 671:1–6.
Larivière S, Jennings AP. 2009. Mustelidae (weasels and relatives). In: Wilson D. E. and Mittermeier R. A., editors. Handbook of the mammals of the world. Vol. 1. Carnivores. Barcelona: Lynx. p. 564–656.
Lodé T. 1999. Comparative measurements of terrestrial and aquatic locomotion in *Mustela lutreola* and *M. putorius*. Z Saugetierkunde 64:110–15.
Morgan CC. 2009. Geometric morphometrics of the scapula of South American caviomorph rodents (Rodentia: Hystricognathi): form, function and phylogeny. Mamm Biol 74:497–506.
Mori K, Suzuki S, Koyabu D, Kimura J, Sung-Yong HAN, Hideki E. 2015. Comparative functional anatomy of hindlimb muscles and bones with reference to aquatic adaptation of the sea otter. J Vet Med Sci 77:571–8.
Moritz S, Fischer MS, Schilling N. 2007. Three-dimensional fibre-type distribution in the paravertebral muscles of the domestic ferret (*Mustela putorius* f. furo) with relation to functional demands during locomotion. Zoology 110:197–211.
Nakajima Y, Endo H. 2013. Comparative humeral microanatomy of terrestrial, semiaquatic, and aquatic carnivorans using micro-focus CT scan. Mamm Study 38:1–8.
Nolet BA, Kruuk H. 1989. Grooming and resting of otters *Lutra lutra* in a marine habitat. J Zool 218:433–40.
Nowak RM. 2005. Walker's carnivores of the world. JHU Press: Baltimore.
R Core Team. 2014. R: a language and environment for statistical computing. Vienna, Austria: R Foundation for Statistical Computing.
Rohlf FJ, Slice D. 1990. Extensions of the Procrustes method for the optimal superimposition of landmarks. Syst Biol 39:40–59.
Rose J, Moore A, Russell A, Butcher M. 2014. Functional osteology of the forelimb digging apparatus of badgers. J Mamm 95:543–58.

Ruff C, Holt B, Trinkaus E. 2006. Who's afraid of the big bad Wolff?: 'Wolff's law' and bone functional adaptation. Am J Phys Anthropol 129:484–98.

Samuels JX, Meachen JA, Sakai SA. 2013. Postcranial morphology and the locomotor habits of living and extinct carnivorans. J Morphol 274:121–46.

Sato JJ, Wolsan M, Prevosti FJ, D'Elía G, Begg C, Begg K, Hosoda T, Campbell KL, Suzuki H. 2012. Evolutionary and biogeographic history of weasel-like carnivorans (Musteloidea). Mol Phylogenet Evol 63:745–57.

Schlager S. 2013. Morpho: calculations and visualizations related to Geometric Morphometrics. R Package Version 21-1141011.

Schmidt-Nielsen K. 1972. Locomotion: energy cost of swimming, flying, and running. Science 177:222–8.

Schmidt-Nielsen K. 1984. Scaling: why is animal size so important? Cambridge University Press: Cambridge.

Schutz H, Guralnick RP. 2007. Postcranial element shape and function: assessing locomotor mode in extant and extinct mustelid carnivorans. Zool J Linn Soc 150:895–914.

Sheffield SR, Thomas HH. 1997. *Mustela frenata*. Mamm Species 570:1–9.

Slater GJ, Harmon LJ, Alfaro ME. 2012. Integrating fossils with molecular phylogenies improves inference of trait evolution. Evolution 66:3931–44.

Taylor MA. 1994. Stone, bone or blubber? Buoyancy control strategies in aquatic tetrapods. Mech Physiol Anim Swim 2:151–61.

Taylor ME. 1989. Locomotor adaptations by carnivores. In: Carnivore behavior, ecology, and evolution. Springer. p. 382–409.

Uhen MD. 2007. Evolution of marine mammals: back to the sea after 300 million years. Anat Rec Adv Integr Anat Evol Biol 290:514–22.

Van Valkenburgh B. 1987. Skeletal indicators of locomotor behavior in living and extinct carnivores. J Vertebr Paleontol 7:162–82.

Veale A. 2013. Observations of stoats (*Mustela erminea*) swimming. N Z J Zool 40:166–9.

Wiley DF, Amenta N, Alcantara DA, Ghosh D, Kil YJ, Delson E, Harcourt-Smith W, Rohlf FJ, St John K, Hamann B. 2005. Evolutionary morphing. In: Proceedings of the IEEE Visualization 2005 (VIS'05). Visualization, 2005. VIS 05. IEEE. IEEE. p. 431–8.

Williams TM. 1983a. Locomotion in the North American mink, a semi-aquatic mammal. II. The effect of an elongate body on running energetics and gait patterns. J Exp Biol 105:283–95.

Williams TM. 1983b. Locomotion in the North American mink, a semi-aquatic mammal. I. Swimming energetics and body drag. J Exp Biol 103:155–68.

Youngman PM. 1990. *Mustela lutreola*. Mamm Species 362:1–3.